30th NENE 2021
September 6 - 9
BLED-SLOVENIA
International Conference Nuclear Energy for New Europe

Scrape-Off Layer Plasma Modelling for the EU DEMO Fusion Reactor with a Liquid Metal Divertor

Giuseppe Francesco Nallo, Fabio Subba, Roberto Zanino
NEMO group, Dipartimento Energia, Politecnico di Torino
Corso Duca degli Abruzzi, 24
10127, Torino, Italy
giuseppefrancesco.nallo@polito.it, fabio.subba@polito.it, roberto.zanino@polito.it

ABSTRACT

Self-healing liquid Metal Divertors (LMDs) are currently being considered among the alternative strategies to address the power exhaust problem in future fusion reactors such as the EU DEMO tokamak. To characterize the power exhaust scenario for a tokamak equipped with an LMD, a self-consistent approach is required, accounting for the mutual interactions between the Scrape-Off Layer (SOL) plasma, the divertor targets and the evaporated metal. To this aim, the SOLPS-ITER code, a 2D multi-fluid solver for the plasma and neutral species, was coupled to a purposely developed LM target erosion/evaporation model and then applied to simulate the EU DEMO plasma in the presence of a liquid Sn divertor.

Calculations considering only D and Sn as plasma (and neutral) species indicates that *vapor shielding* arising from the interactions of the eroded/evaporated metal with the near-surface plasma effectively mitigates the target heat flux, reducing the computed peak value from $\sim 60\ \mathrm{MW/m^2}$ (computed for a pure D case, mimicking a solid divertor) to $\sim 44\ \mathrm{MW/m^2}$. However, this value is still larger than the power handling limit of $\sim 40\ \mathrm{MW/m^2}$ for the considered LMD design. Moreover, the computed Sn concentration in the core plasma was close to the estimated compatibility limit of $\sim 0.05\%$. These results motivated further simulations considering the injection of Ar in the SOL plasma to radiate part of the plasma power before it reaches the target, also leading to a reduced erosion/evaporation rate. The results indicated a significant widening of the operational window for the EU DEMO equipped with an LMD using Sn, both in terms of tolerable target heat fluxes and in terms of core plasma contamination.

1 INTRODUCTION

1.1 The power exhaust problem in future fusion reactors

Nuclear fusion has the potential to provide almost unlimited, carbon-free electricity without producing long-lived radioactive waste. The most promising fusion reactor concept is the *tokamak*, involving the confinement of a hot, ionized gas (the *plasma*) by means of magnetic fields. The arrangement of magnetic field lines is such that two regions can be distinguished: the central *core* plasma, hotter than the sun (~ 100 MK), where fusion reactions occur, and the colder *edge* plasma or *scrape-off layer (SOL)*, where magnetic field lines intersect purposely engineered solid surfaces (the *divertor targets*). Due to the anisotropy of plasma transport, which occurs preferentially *along* magnetic field lines, the wetted area available for the plasma to strike on the divertor targets is relatively small, resulting in significant heat and particle fluxes.

This can lead to melting and erosion, threatening both the integrity of the Plasma-Facing Surface (PFS) and the core plasma performance, since eroded particles cause harmful core plasma radiation which could hinder the fusion process.

The strategy envisaged for the next-step fusion device (the ITER experiment, currently under construction in Cadarache, France) foresees the use of actively cooled tungsten (W) *monoblocks* as divertor targets, in combination with the injection of impurities (e.g. Ar) in the SOL to isotropically radiate part of the plasma power *before* it reaches the target, leading to partial or total *plasma detachment*. However, the extrapolation of this solution to future fusion reactors such as the EU DEMO, whose pre-conceptual design is ongoing within the EUROfusion consortium, see Figure 1 (left), is subject to considerable uncertainties, mainly due to the larger amount of energy stored in the core plasma and to the presence of significant neutron irradiation [1]. To address this challenging power exhaust problem, alternative solutions are being studied, including self-healing Liquid Metal Divertors (LMDs), and a dedicated experiment, the Divertor Tokamak Test (DTT), will shortly begin construction at ENEA Frascati, Italy [2].

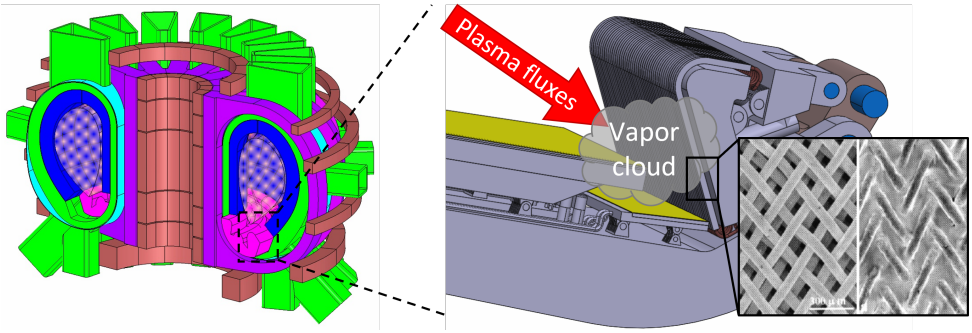

Figure 1: CAD of the EU DEMO [3] (left), and detail of the outboard divertor target [4], with a sketch of the vapor shielding effect and a picture of a CPS before and after wetting [5] (right).

1.2 A possible solution: liquid metal divertors

The key strength of LMDs is represented by the self-healing nature of a liquid Plasma-Facing Surface (PFS), as opposed to a solid one. Indeed, material losses - which, for an LMD, are due not only to plasma-induced erosion but also to evaporation - can be compensated for by continuously replenishing the PFS with fresh LM. By adopting an LM-filled Capillary-Porous Structure (CPS) as PFS, capillary forces can be exploited to passively "pump" the LM from a heated reservoir to the exposed surface, thus providing the required replenishment – as in a candle wick [6], see Figure 1 (right). Experiments in both Linear Plasma Devices (LPDs) and in tokamaks have confirmed the capability of a CPS placed on an actively cooled substrate to withstand reactor-relevant plasma fluxes without significant damage to the porous matrix nor to the substrate, while preventing electromagnetic forces from tearing the LM layer apart. Moreover, it was observed that the metal released from the target via erosion/evaporation (hereafter called *vapor* for simplicity) interacts with the near-target plasma leading to an intrinsic mitigation of the power reaching the divertor - the *vapor shielding* effect [7], schematically indicated in Figure 1 (right). On the other hand, the large unmitigated plasma heat fluxes foreseen for the EU DEMO will cause the release of a significant amount of vapor. The latter, once ionized, can reach the core plasma, depending on the balance between friction and thermal forces, leading to excessive dilution (in the case of low-Z LMs such as Li) and/or radiation (in the case of high-Z LMs such as Sn).

1.3 The need for self-consistent models

Assessing the balance between the beneficial heat load mitigation related to vapor shielding and the possible negative impact on core plasma performance is essential to characterize the power exhaust scenario for a tokamak adopting an LMD. To this aim, self-consistent models are required, accounting for the mutual interactions between plasma, target and vapor.

The self-consistent simulation of the tokamak plasma in the presence of an LMD was performed in the past via both simplified (0D or 1D) models [8, 9] and more detailed (2D) edge plasma codes such as TECXY [10]. In the work here reported, SOLPS-ITER, a state-of-the-art 2D multi-fluid code for plasma and neutral species, was coupled to a model for the target erosion and applied to the EU DEMO plasma equipped with an LMD using Sn, with the aim of identifying a viable operational window, also considering the effectiveness of seeding Ar in the SOL to provide further heat load mitigation.

2 SYSTEM DESCRIPTION

2.1 Vessel shape and magnetic equilibrium

The wall geometry and magnetic equilibrium here considered are consistent with [11], corresponding to the 2017 EU DEMO design. In compliance with the currently adopted strategy for developing LMD concepts within EUROfusion, the geometry and magnetic equilibrium were left unchanged, only replacing the solid (W) divertor targets with a liquid Sn-filled CPS.

2.2 Liquid metal target

In this work, the liquid Sn target design recently developed at ENEA Frascati was considered [12]. Consistently with the baseline, the the toroidal extension of the divertor is subdivided into 48 *cassettes*. To cover the entire surface of both inboard and outboard divertor targets for each cassette, in place of the baseline W monoblocks, LMD *modules* are juxtaposed and connected hydraulically in parallel. The CAD of a single module is shown in Figure 2 (left).

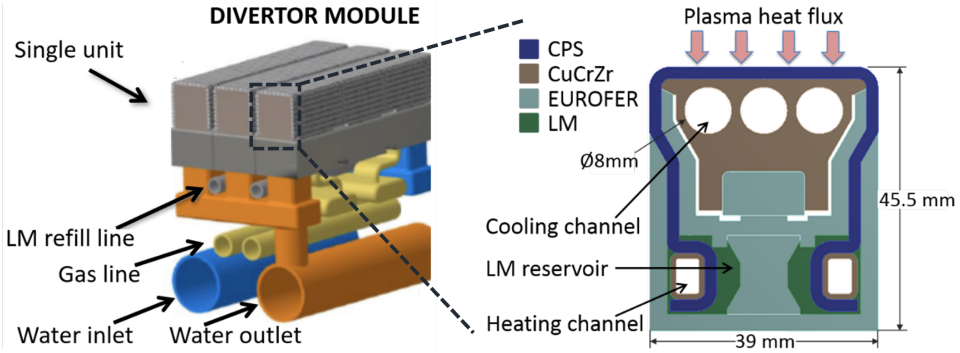

Figure 2: CAD of the divertor module, adapted from [2] (left), and cross section of the divertor unit, adapted from [12] (right) for the ENEA design.

For each module, the plasma-facing element is represented by three units, hydraulically connected in parallel, see Figure 2 (right). Each unit is covered by a 2 mm-thick CPS placed on top of a CuCrZr heat sink, actively cooled by pressurized water (50 bar) flowing in cooling channels. Preliminary calculations indicated that heat fluxes as large as ~ 40 MW/m^2 can be tolerated by this design, the limiting factor being the Critical Heat Flux (CHF) to the coolant.

3 PHENOMENOLOGY

3.1 Target erosion/evaporation mechanisms

Material loss processes for an LM target can be subdivided into plasma-induced erosion, i.e. *sputtering*, and evaporation. Physical sputtering (which also occurs for a solid surface) is caused by momentum transfer from energetic plasma ions to wall atoms, and depends on the flux and energy of the incoming particles (the projectiles) and on the projectile-target combination. Thermal sputtering is instead specific of liquid surfaces, as it arises from the formation of loosely bound *adatoms* following from plasma impact, which are then easily evaporated/sublimated - thus implying a dependence on the surface temperature [13]. Evaporation is instead only dependent on the target temperature, which is ultimately determined by the combination of plasma heat flux and active cooling strategy adopted for the target. The *net* erosion rate associated to these processes is reduced by a factor$\sim 10^2$ by *prompt redeposition* of emitted particles which are ionized within the first gyro-radius [14].

It should be noticed that, following from plasma impact, fuel (D/T) neutrals arise from the target after having been neutralized, and re-emitted at thermal energies - the *recycling* process.

3.2 Plasma-vapor interactions

The near-surface plasma interacts with the emitted vapor via several mechanisms, schematically represented in Figure 3 (right). The plasma electrons can *ionize* the vapor, leading to the formation of increasingly charged ions. At sufficiently low plasma temperatures, these ions can *recombine*, i.e. can be neutralized again. Another relevant process, responsible for the plasma-neutral friction, is the *charge-exchange* between hot plasma and cold neutrals. Moreover, the vapor - and the successively ionized metal - *radiates* via both Bremsstrahlung and line radiation, a process which is beneficial in the SOL but harmful in the core.

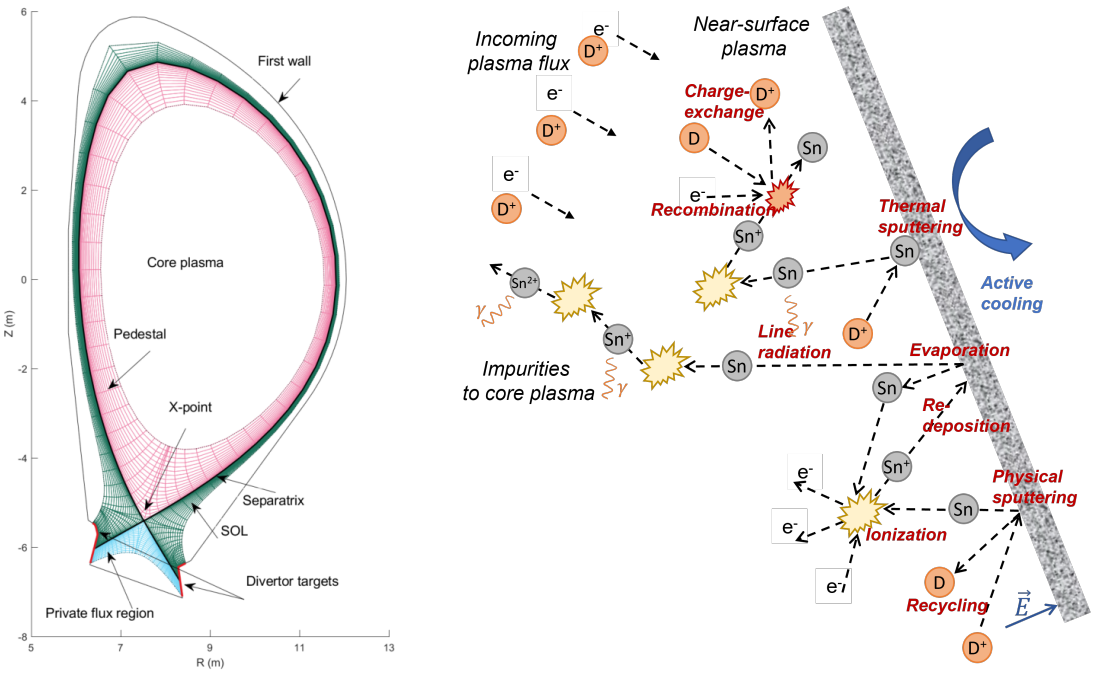

Figure 3: Computational grid used for the SOLPS-ITER calculations, with the most relevant plasma regions indicated [14] (left), and sketch of the plasma-vapor-target interactions (right).

It should be noticed that the same processes occur as a results of plasma interacting with fuel neutrals arising from recycling and with purposely seeded impurities such as Ar.

4 MODEL DESCRIPTION

4.1 SOL plasma and vapor: SOLPS-ITER simulation setup

The SOLPS-ITER 2D multi-fluid code, assuming toroidal symmetry, was applied to simulate the full set of both ionized species (i.e. D^+, Sn^+, Sn^{2+}, ..., Sn^{50+}, and possibly Ar^+, Ar^{2+}, ..., Ar^{18+}) and neutral species (D^0, Sn^0 and possibly Ar^0) [15]. Using a fluid model for the neutrals instead of the more accurate kinetic model available in SOLPS-ITER (based on the EIRENE code) allowed to perform relatively inexpensive parametric scans, while still allowing for an accurate description of the collisional. However, this approach does not allow to fully characterize the particle exhaust scenario (especially in terms of He ash), which is left for future work. The computational grid extends inside the *separatrix* (the magnetic field line separating the core and SOL) to include the pedestal region, and outside the separatrix to include several power decay lengths, see Figure 3 (left). Parallel transport is classical, whereas perpendicular transport is anomalous, with diffusion coefficients consistent with [11]. 100% fuel recycling at the target was assumed. Atomic data for Sn were obtained as a courtesy of Dr. O'Mullane [16], but will soon be made available in the official ADAS database [17].

4.2 External module for surface temperature and target erosion rate

A 2D FEM thermal model of the singe unit of the the ENEA liquid Sn divertor design was developed and coupled to SOLPS-ITER, to self-consistently evaluate the target temperature profile. This profile, together with the distribution of the impinging plasma energy and fluxes, was adopted to determine the eroded/evaporated particle flux from the target, which represents a boundary source for the SOLPS-ITER neutral model.

5 RESULTS

5.1 Simulation matrix

A first set of cases considering only D+Sn were performed, varying the outboard midplane electron density at the separatrix $n_{e,sep}$ between $3.5 \cdot 10^{19}$ m^{-3} and $4.5 \cdot 10^{19}$ m^{-3}, corresponding to 40% - 52% of the Greenwald density, to study different reactor operating conditions. A second set of cases was then performed considering D+Sn+Ar, injecting Ar from the outer boundary of the calculation domain with a uniform distribution, to obtain a total injection rate $\Gamma_{Ar} = 5 \cdot 10^{20}$ s^{-1}, $7 \cdot 10^{20}$ s^{-1} and $1 \cdot 10^{21}$ s^{-1}, to mitigate the target heat flux without making Ar itself a threat for the core plasma purity. The power crossing the separatrix was fixed to 150MW. Table 1 reports the identification number within the MDSplus database corresponding to each simulated case, to promote reproducibility of the results.

Table 1: Summary of the simulations performed, with the corresponding MDSplus IDs.

		$n_{e,sep} = 3.5 \cdot 10^{19}$ m^{-3}	$n_{e,sep} = 3.75 \cdot 10^{19}$ m^{-3}	$n_{e,sep} = 4.0 \cdot 10^{19}$ m^{-3}	$n_{e,sep} = 4.25 \cdot 10^{19}$ m^{-3}	$n_{e,sep} = 4.5 \cdot 10^{19}$ m^{-3}
D+Sn		182222	182223	182398	182399	182226
D+Sn+Ar	$\Gamma_{Ar} = 5 \cdot 10^{20}$ s^{-1}	182233	182234	182235	182330	182237
	$\Gamma_{Ar} = 7 \cdot 10^{20}$ s^{-1}	182238	182239	182246	182241	182242
	$\Gamma_{Ar} = 1 \cdot 10^{21}$ s^{-1}	182444	182445	182229	182230	182231

5.2 Power balance and erosion rates

Figure 4 (left) shows that, for the D+Sn case, Sn is responsible for significant SOL radiation. By seeding increasingly large amounts of Ar, the SOL power balance becomes instead dominated by Ar radiation. This indicates that the plasma heat load mitigation provided by Ar along the SOL causes a reduction of the heat flux reaching the target, thus inducing a lower erosion rate, as confirmed by Figure 4 (right). In other words, the intrinsic target self-protection associated to vapor shielding in front of the target and along the SOL due to Sn radiation, see Figure 5 (left), is replaced by Ar seeding along the SOL, i.e. upstream with respect to the target. As a result, the target no longer operates in a "vapor shielding" regime, but rather in a low erosion/evaporation regime which is similar to the one of a solid divertor, see Figure 5 (right).

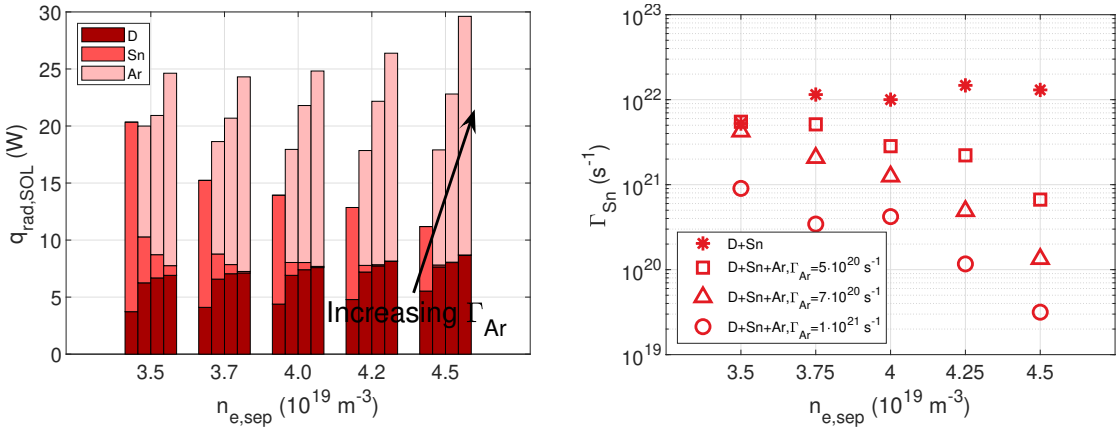

Figure 4: Computed radiated power in the SOL due to the various plasma and neutral species (left), and total Sn erosion/evaporation rate (right), for the entire set of $n_{e,sep}$ and Γ_{Ar}.

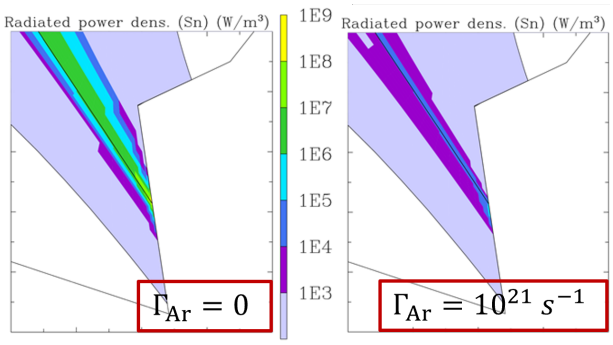

Figure 5: Computed Sn radiation density distribution in front of the outboard target.

5.3 Target heat flux and core plasma contamination

The target heat flux mitigation caused by vapor shielding is evident from the difference between the solid black and red curves in Figure 6 (left), representing the pure D and D+Sn cases, respectively. However, only seeding Ar it was possible to obtain a sufficiently large margin from the estimated maximum tolerable heat flux.

As far as the core plasma compatbility is concerned, Figure 6 (right) indicates that the reduced material losses caused by Ar seeding effectively reduces the core plasma contamina-

tion, leading to a promising operational window which is compliant with the tolerability limits previosly estimated via COREDIV calculations [18].

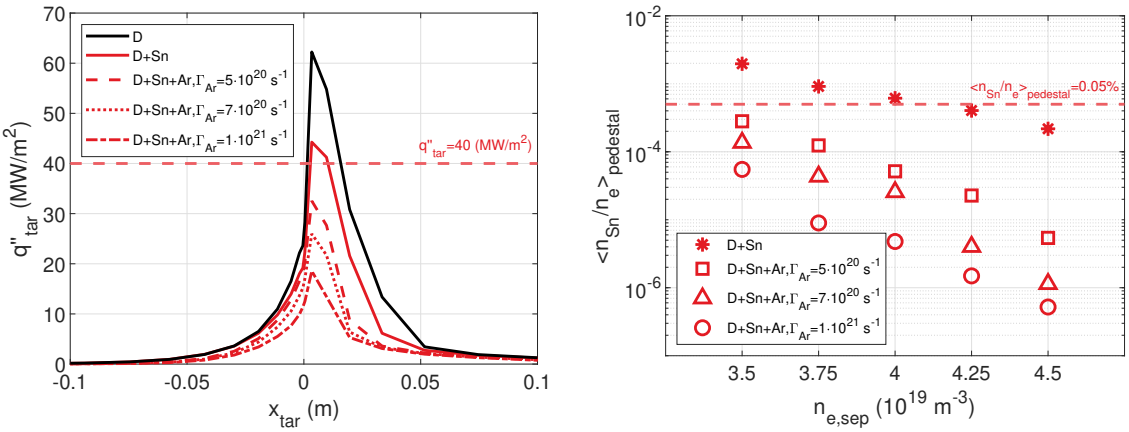

Figure 6: Computed outboard target heat flux profiles (left) and core Sn concentration (right) for the entire set of $n_{e,sep}$ and Γ_{Ar}. The solid black line in the left plot refers to a pure D case (without vapor shielding). Horizontal dashed lines indicate estimated tolerability limits.

6 CONCLUSION AND PERSPECTIVE

In this paper, a novel self-consistent methodology was applied to simulate the EU DEMO tokamak equipped with a liquid Sn divertor, including the most relevant physical processes. Simulations without Ar indicate that, notwithstanding the significant load mitigation due to vapor shielding, the target peak heat flux could still be large enough to damage the CPS, and the eroded/evaporated metal could induce intolerable core plasma contamination. Simulations with Ar seeding indicate that Ar radiation in the SOL effectively replaces vapor shielding, thus reducing the material losses and core plasma contamination while further mitigating the target heat flux. These encouraging results suggest the existence of an operational scenario for the EU DEMO with a self-healing LMD, characterized by negligible material losses.

In perspective, more refined modelling including a kinetic neutral model and integrated target-SOL-core simulations is envisaged, together with experimental validation against experiments in both LPDs and tokamaks.

ACKNOWLEDGMENTS

This work has been carried out within the framework of the EUROfusion Consortium and has received funding from the Euratom research and training programme 2014–2018 and 2019-2020 under grant agreement No 633053. The views and opinions expressed herein do not necessarily reflect those of the European Commission. The authors gratefully acknowledge fruitful discussions with Dr. G. Mazzitelli, Dr. D. Coster and Mr. M. Moscheni.

REFERENCES

[1] A. J. Donné, European Research Roadmap to the Realisation of Fusion Energy, EUROfusion, 2018.

[2] A. Pizzuto, DTT Divertor Tokamak Test Facility Interim Design Report (green book), ENEA, 2019.

[3] B. Koncar, O. Costa Garrido, M. Draksler, R. Brown, M. Coleman, "Initial optimization of DEMO fusion reactor thermal shields by thermal analysis of its integrated systems", Fus. Eng. Des., 125, 2017, pp. 38-49.

[4] B. Meszaros, EU DEMO 2015 - DEMO TOKAMAK COMPLEX, EUROfusion technical report, 2015.

[5] G. Mazzitelli, M. L. Apicella, M. Iafrati, G. Apruzzese, F. Bombarda et al., "Experiments on the Frascati Tokamak Upgrade with a liquid tin limiter", Nucl. Fus., 59, 2019, 096004 (8 pp).

[6] S. V. Mirnov, V. A. Evtikhin, "The tests of liquid metals (Ga, Li) as plasma facing components in T-3M and T-11M tokamaks", Fus. Eng. Des., 81, 2006, pp. 113-119.

[7] G. Van Eden, V. Kvon, M. C. M. van de Sanden, T. W. Morgan, "Oscillatory vapour shielding of liquid metal walls in nuclear fusion devices", Nat. Comm., 8, 2017, 192 (10 pp).

[8] G. F. Nallo, G. Mazzitelli, L. Savoldi, F. Subba, R. Zanino, "Self-consistent modelling of a liquid metal box-type divertor with application to the divertor tokakak test facility: Li versus Sn", Nucl. Fuc., 59, 2019, 066020 (17 pp).

[9] E. Marenkov, A. Pshenov, "Vapor shielding of liquid lithium divertor target during steady state and transient events", Nucl. Fus., 60, 2020, 026011 (12 pp).

[10] V. Pericoli Ridolfini, R. Ambrosino, S. Mastrostefano, P. Chmielewski, M. Poradzinski, R. Zagorski, "A comparative study of the effects of liquid lithium and tin as DEMO divertor targets on the heat loads and SOL properties", Phys. Plasmas, 26, 2019, 012507 (13 pp).

[11] F. Subba, L. Aho-Mantila, D. Coster, G. Maddaluno, G. F. Nalo et al., "Modelling of mitigation of the power divertor loading for the EU DEMO through Ar injection", Plasma Phys. Control. Fusion, 60, 2018, 035013 (9 pp).

[12] S. Roccella, G. Dose, R. de Luca, M. Iafrati, A. Mancini, G. Mazzitelli, "CPS Based Liquid Metal Divertor Target for EU-DEMO", J. Fusion Energy (17 pp).

[13] R.P. Doerner, S.I. Krasheninnikov, K. Schmid, "Particle-induced erosion of materials at elevated temperature", J. Appl. Phys., 95, 2004, pp. 4471-4475.

[14] G. F. Nallo, Modelling liquid metals for nuclear fusion and fission reactors, Ph.D. thesis, Politecnico di Torino, 2021.

[15] S. Wiesen, D. Reiter, V. Kotov, M. Baelmans, W. Dekeyser et al., "The new SOLPS-ITER code package", J. Nucl. Mat., 463, 2015, pp. 480-484.

[16] M. O'Mullane, D. Coster, Private Communication, 2019.

[17] H.P. Summers, The ADAS User Manual, version 2.6, 2004.

[18] V. Pericoli Ridolfini, P. Chmielewski, I. Ivanova-Stanik, M. Poradzinski, R. Zagorski et al., "Comparison between liquid lithium and liquid tin targets in reactor relevant conditions for DEMO and I-DTT", Phys. Plasmas, 27, 2020, 112506 (11 pp).